Journal of Mathematical Modeling
Vol. 13, No. 4, 2025, pp. 823-840. Research Article

JMM

Non-standard finite difference scheme for system of singularly perturbed Fredholm integro-differential equations

P. Antony Prince[†], **Lolugu Govindarao**[†*], **Sekar Elango**[†]

[†]*Department of Mathematics, Amrita School of Physical Science, Coimbatore, Amrita Vishwa Vidyapeetham, India*
Email(s): p_antonyprince@cb.students.amrita.edu, l_govindarao@cb.amrita.edu, e_sekar@cb.amrita.edu

Abstract. This article solves computationally a system of reaction-diffusion singularly perturbed Fredholm integro-differential equations. A non-standard finite difference approach applies the derivative components, whereas the composite trapezoidal rule handles the integral components. The proposed computational method for a system of reaction-diffusion singularly perturbed Fredholm integro-differential equations exhibits a convergence rate of order two. An computational example is provided to substantiate the efficacy of the theoretical results.

Keywords: Singular perturbation, coupled system, fitted operator, Fredholm integral, boundary layer.
AMS Subject Classification 2010: 65G50, 65L12, 65L70, 65R20.

1 Introduction

The solution of the integro-differential equations (IDEs) has facilitated numerous scientific computations. They serve crucial functions across various scientific disciplines, including aerodynamics, chemistry, economics, electronics and electricity, oceanography, hydrodynamics and industrial networks [6, 33]. In [2], Malay Banerjee presents a neural field model on nonlocal reaction-difusion equations in biomedical applications. The model is

$$\frac{\partial u}{\partial t} = D_1 \frac{\partial^2 u}{\partial t^2} + W_1 - W_2 - \sigma_1 u,$$
$$\frac{\partial v}{\partial t} = D_2 \frac{\partial^2 v}{\partial t^2} + W_3 - W_4 - \sigma_1 v,$$

*Corresponding author
Received: 29 April 2025/ Revised: 24 May 2025/ Accepted: 27 May 2025
DOI: 10.22124/jmm.2025.30538.2740

where

$$W_k = \begin{cases} \int\limits_{-\infty}^{\infty} \Psi_k(x-y)\, S_k(u(y,t))\, dt, & k = 1 \text{ and } 3, \\ \int\limits_{-\infty}^{\infty} \Psi_k(x-y)\, S_k(v(y,t))\, dt, & k = 2 \text{ and } 4, \end{cases}$$

u is the activating signals, and v is inhibiting signals, these integral terms characterize signal transmission via the axons from all locations y to a specified position x, $\Psi_k(x-y)$ are exponentially decaying positive connectivity functions that represent the density of connections as a function of distance and $S_k(u), S_k(v)$ are represent the response functions of sigmoid neurons to activating and inhibiting signals, respectively. Based on the above model, our objective is to present a system of reaction-diffusion singularly perturbed Fredholm integro-differential equations (SPFIDEs).

Consider a system of second-order SPFIDEs for finding $\overrightarrow{\mathbf{u}}(t) \in C^2(\bar{\Omega})$ such that

$$\begin{cases} \mathfrak{L}_{\varepsilon_1,\varepsilon_2} \overrightarrow{\mathbf{u}}(t) := \mathfrak{L}_1 \overrightarrow{\mathbf{u}}(t) + \mathfrak{L}_2 \overrightarrow{\mathbf{u}}(t) = \overrightarrow{\mathbf{f}}(t),\ t \in (0,1) = \Omega, \\ \overrightarrow{\mathbf{u}}(0) = \begin{pmatrix} u_1(0) \\ u_2(0) \end{pmatrix}, \quad \overrightarrow{\mathbf{u}}(1) = \begin{pmatrix} u_1(1) \\ u_2(1) \end{pmatrix}, \end{cases} \tag{1}$$

where $\mathfrak{L}_1 \overrightarrow{\mathbf{u}}(t) = \begin{pmatrix} -\varepsilon_1 \frac{d^2}{dt^2} & 0 \\ 0 & -\varepsilon_2 \frac{d^2}{dt^2} \end{pmatrix} \overrightarrow{\mathbf{u}}(t) + \mathbb{A}(t) \overrightarrow{\mathbf{u}}(t),\ \mathfrak{L}_2 \overrightarrow{\mathbf{u}}(t) = \lambda \int\limits_0^1 \Theta(t,z) \overrightarrow{\mathbf{u}}(z)\, dz,$

$$\overrightarrow{\mathbf{u}}(t) = \begin{pmatrix} u_1(t) \\ u_2(t) \end{pmatrix},\ \mathbb{A}(t) = \begin{pmatrix} a_{11}(t) & a_{12}(t) \\ a_{21}(t) & a_{22}(t) \end{pmatrix},\ \overrightarrow{\mathbf{f}}(t) = \begin{pmatrix} f_1(t) \\ f_2(t) \end{pmatrix}.$$

Here, for $i, j = 1, 2$, $f_i(t), a_{ij}(t)$ are sufficiently smooth functions and $0 < \varepsilon_1 \le \varepsilon_2 \ll 1$, λ is real parameter and $\Theta(t,z)$ is a kernel function for $(t,z) \in \bar{\Omega} \times \bar{\Omega}$.

To ensure that $\mathfrak{L}_{\varepsilon_1,\varepsilon_2} \overrightarrow{\mathbf{u}}(t)$ adheres to a standard comparison principle, it is assumed that

$$\begin{aligned} & a_{11}(t) > |a_{12}(t)|, \quad a_{22}(t) > |a_{21}(t)|, \quad t \in \bar{\Omega}, \\ & a_{12}(t) \le 0, \quad a_{21}(t) \le 0, \quad t \in \bar{\Omega}, \\ & \min\{a_{11}(t) + a_{12}(t), a_{21}(t) + a_{22}(t)\} \ge \delta > 0. \end{aligned}$$

Singularly perturbed differential equations (SPDEs) are typically defined as differential equations that are generated by multiplying a tiny parameter with the higher derivative term of a differential equation. Such a parameter is known as the singular perturbation parameter. The solutions to these equations provide a thin layer known as a boundary layer within the domain. In solving SPDEs, standard approaches utilizing uniform step sizes yield inaccurate results. They are unstable and inappropriate in most situations [9, 14, 21, 22, 28–30]. Consequently, numerous researchers numerically approach SPDEs in [7, 10, 16, 31, 32]. Lange and Smith [18] derived the existence and uniqueness of SPFIDEs. Cimen et al. [4] used interpolating quadrature rules to compute SPFIDEs with boundary values. A numerical solution for the non-linear first-order singularly perturbed Volterra IDEs developed by Sevgin [35]. Amiraliyev et al. [1] developed a method to calculate error estimates that are consistent across different parameters for estimating solutions of first-order SPFIDEs with uniform mesh. Durmaz et al. [8]

tackled the second-order reaction-diffusion SPFIDEs utilizing a fitted difference scheme on a Shishkin mesh. Afterwards, it attained a non-optimal rate of convergence in the second order. Panda et al. [25, 26] solved SPFIDEs for the linear and nonlinear cases. Elango et al. [11–13, 24] successfully solved the second-order reaction-diffusion and convection-diffusion SPFIDEs. Govindarao et al. [15] handled the reaction-diffusion SPFIDEs with integral boundary conditions. Priyadarshana et al. used adaptive grid algorithms to solve singularly perturbed second-order Volterra integro differential equations [27]. A multitude of techniques exists for resolving a system of integro-differential equations [34], the Adomian decomposition method [3] and the variational iteration method [36]. To solve the system of SPFIDEs, special techniques such as those used for SPDEs are required. Due to the small parameters ε's multiplying the higher order differential equations, the standard finite difference is inaccurate for solutions with tiny parameter values. In this context, the Non-Standard Finite difference(NSFD) method is employed as an effective approach to solve a system of SPFIDEs with high accuracy.

This article aims to achieve a convergence rate of order two for the system of second-order SPFIDEs. Initially, an NSFD scheme is employed for the derivative part, whereas the composite trapezoidal rule is utilized for the integral component on a uniform grid. Consequently, the convergence rate of order two corresponds to equation (1) with a finite number of mesh points. The global convergence rate of order two is demonstrated computationally.

This is a brief overview of the manuscript's layout. Section 2 presents the theoretical estimates of the system of SPFIDEs. In Section 3, the mesh is constructed and the problem is numerically discretized to obtain an approximation. The proof that shows our method is accurate with the convergence of order two is given in Section 4. The findings are encapsulated, and the convergence sequence together with pointwise errors are validated by numerical example in Section 5. The conclusion in Section 6 and the appendix include additional findings for $m-$systems of equations.

2 Theoretical estimates

This section considers the system of SPFIDEs of the form (1) and discusses its stability.

Lemma 1 (**Maximum principle**). *Let* $\overrightarrow{\mathbf{u}}(t) \in C^2(\bar{\Omega})$ *and* $|\lambda| \leq \frac{\delta}{\max\limits_{0\leq t\leq 1}\int_0^1 |\Theta(t,z)|dz}$, *with* $\overrightarrow{\mathbf{u}}(0) \geq 0$, $\overrightarrow{\mathbf{u}}(1) \geq 0$, $\mathfrak{L}_{\varepsilon_1,\varepsilon_2}\overrightarrow{\mathbf{u}}(t) \geq 0$, $\forall\, t \in \Omega$. *Then* $\overrightarrow{\mathbf{u}}(t) \geq 0$, $\forall\, t \in \bar{\Omega}$.

Proof. Let $\chi_1(l) = \min\limits_{\bar{\Omega}} \chi_1$ and $\chi_2(m) = \min\limits_{\bar{\Omega}} \chi_2$. Consider

$$\begin{pmatrix} -\varepsilon_1 \frac{d^2}{dt^2} & 0 \\ 0 & -\varepsilon_2 \frac{d^2}{dt^2} \end{pmatrix} \overrightarrow{\mathbf{u}}(t) + \mathbb{A}(t)\overrightarrow{\mathbf{u}}(t) = \overrightarrow{\mathbf{f}}(t) - \lambda \int_0^1 \Theta(t,z)\overrightarrow{\mathbf{u}}(z)\,dz, \tag{2}$$

and assume that without loss of generality $\chi_1(l) \leq \chi_2(m)$. Also, assume $\chi_1(l) < 0$, which leads to a contradiction. Observe that $l \neq 0,1$ and that $\chi_1''(l) \geq 0$. The first component of equation (2) is expressed as

$$-\varepsilon_1\chi_1''(l) + a_{11}\chi_1(l) + a_{12}\chi_2(l) = -\varepsilon_1\chi_1''(l) + (a_{11}+a_{12})\chi_1(l) + (\chi_2(l)-\chi_1(l))a_{12}.$$

Therefore, the first component is strictly negative. It is a contradiction to the condition $\mathfrak{L}_{\varepsilon_1,\varepsilon_2}\overrightarrow{\mathbf{u}}(t) \geq 0$. $\square$

Lemma 2 (Stability). *Let $\overrightarrow{\mathbf{u}}(t)=(u_1,u_2)^T$ be the solution of $\mathfrak{L}_{\varepsilon_1,\varepsilon_2}\overrightarrow{\mathbf{u}}(t)$. If $\frac{\partial^p\Theta(t,z)}{\partial t^p}\in C([0,1]\times[0,1])$ for $p=0,1,2,3,4$ and $f_i(t)$, $a_{ij}(t)$ are $C^2[0,1]$ for $i,j=1,2$. Then there exists an independent constant C of ε_1 and ε_2 such that*

$$
\begin{aligned}
|u_1(t)| &\le C\left[1+\mathscr{D}_{\varepsilon_2}(t)\right],\\
|u_2(t)| &\le C\left[1+\mathscr{D}_{\varepsilon_2}(t)\right],\\
|u_1^{(p)}(t)| &\le C\left[1+\varepsilon_1^{\frac{-p}{2}}\mathscr{D}_{\varepsilon_1}(t)+\varepsilon_2^{\frac{-p}{2}}\mathscr{D}_{\varepsilon_2}(t)\right], \quad \text{for } p=1,2,3,4,\\
|u_2^{(p)}(t)| &\le C\left[1+\varepsilon_2^{\frac{-p}{2}}\mathscr{D}_{\varepsilon_2}(t)\right], \quad \text{for } p=1,2,\\
|u_2^{(p)}(t)| &\le C\left[1+\frac{1}{\varepsilon_2}\left(\varepsilon_1^{\frac{(2-p)}{2}}\mathscr{D}_{\varepsilon_1}(t)+\varepsilon_2^{\frac{(2-p)}{2}}\mathscr{D}_{\varepsilon_2}(t)\right)\right], \quad \text{for } p=3,4,
\end{aligned}
$$

where

$$
\begin{aligned}
\mathscr{D}_{\varepsilon_1}(t) &= e^{\left(-t\sqrt{\frac{\delta}{\varepsilon_1}}\right)}+e^{\left(-(1-t)\sqrt{\frac{\delta}{\varepsilon_1}}\right)},\\
\mathscr{D}_{\varepsilon_2}(t) &= e^{\left(-t\sqrt{\frac{\delta}{\varepsilon_2}}\right)}+e^{\left(-(1-t)\sqrt{\frac{\delta}{\varepsilon_2}}\right)}.
\end{aligned}
$$

Proof. The solution of equation (1) is in the form of $\overrightarrow{\mathbf{u}}(t)=\overrightarrow{\mathbf{v}}(t)+\overrightarrow{\mathbf{w}}_L(t)+\overrightarrow{\mathbf{w}}_R(t)$, where $\overrightarrow{\mathbf{v}}(t)$ is the regular component, $\overrightarrow{\mathbf{w}}_L(t)$ is the left singular component, and $\overrightarrow{\mathbf{w}}_R(t)$ is the right singular component. Now the regular component $\overrightarrow{\mathbf{v}}(t)$ is the solution of the equation

$$
\mathfrak{L}_{\varepsilon_1,\varepsilon_2}\overrightarrow{\mathbf{v}}(t):=\begin{pmatrix}-\varepsilon_1\frac{d^2}{dt^2} & 0\\ 0 & -\varepsilon_2\frac{d^2}{dt^2}\end{pmatrix}\overrightarrow{\mathbf{v}}(t)+\mathbb{A}(t)\overrightarrow{\mathbf{v}}(t)=\overrightarrow{\mathbf{f}}(t)-\lambda\int_0^1\Theta(t,z)\overrightarrow{\mathbf{v}}(z)\,dz.
$$

Let us take the barrier function

$$
\overrightarrow{\Psi^{\pm}}(t)=\frac{1}{\delta}\|\overrightarrow{\mathbf{f}}(t)\|+\|\overrightarrow{\mathbf{v}}(0)\|+\|\overrightarrow{\mathbf{v}}(1)\|+\left\|\lambda\int_0^1\Theta(t,z)\overrightarrow{\mathbf{v}}(z)\,dz\right\|\pm\overrightarrow{\mathbf{v}}(t).
$$

The subsequent inequalities are satisfied

$$
\overrightarrow{\Psi^{\pm}}(0)\ge 0 \quad \text{and} \quad \overrightarrow{\Psi^{\pm}}(1)\ge 0.
$$

Furthermore

$$
\mathfrak{L}_{\varepsilon_1,\varepsilon_2}\overrightarrow{\Psi^{\pm}}(t)=\left\{\begin{array}{r}
\|f_1(t)\|\dfrac{(a_{11}(t)+a_{12}(t))}{\delta}+(a_{11}(t)+a_{12}(t))\left(\|v_1(0)\|+\|v_1(1)\|\right)\\
+(a_{11}(t)+a_{12}(t))\left\|\lambda\displaystyle\int_0^1\Theta(t,z)v_1(z)\,dz\right\|\\
\|f_2(t)\|\dfrac{(a_{21}(t)+a_{22}(t))}{\delta}+(a_{21}(t)+a_{22}(t))\left(\|v_2(0)\|+\|v_2(1)\|\right)\\
+(a_{21}(t)+a_{22}(t))\left\|\lambda\displaystyle\int_0^1\Theta(t,z)v_2(z)\,dz\right\|
\end{array}\right\}\pm\mathfrak{L}_{\varepsilon_1,\varepsilon_2}\overrightarrow{\mathbf{v}}(t)
$$

$$\begin{aligned}&\geq \|\overrightarrow{\mathbf{f}}(t)\| + \delta\left(\|\overrightarrow{\mathbf{v}}(0)\| + \|\overrightarrow{\mathbf{v}}(1)\|\right) + \delta\left\|\lambda\int_0^1 \Theta(t,z)\overrightarrow{\mathbf{v}}(z)\,dz\right\| \\ &\pm\left[\overrightarrow{\mathbf{f}}(t) - \lambda\int_0^1 \Theta(t,z)\overrightarrow{\mathbf{v}}(z)\,dz\right] \geq 0.\end{aligned}$$

Therefore $\mathfrak{L}_{\varepsilon_1,\varepsilon_2}\overrightarrow{\Psi^{\pm}}(t) \geq 0$. By applying the maximum principle

$$\overrightarrow{\mathbf{v}}(t) \leq \frac{1}{\delta}\|\overrightarrow{\mathbf{f}}(t)\| + \|\overrightarrow{\mathbf{v}}(0)\| + \|\overrightarrow{\mathbf{v}}(1)\| + \left\|\lambda\int_0^1 \Theta(t,z)\overrightarrow{\mathbf{v}}(z)\,dz\right\|,$$

then

$$\begin{aligned}\overrightarrow{\mathbf{v}}(t) &\leq \frac{1}{\delta}\|\overrightarrow{\mathbf{f}}(t)\| + \|\overrightarrow{\mathbf{v}}(0)\| + \|\overrightarrow{\mathbf{v}}(1)\| + |\lambda|\max_{0\leq t\leq 1}\int_0^1 |\Theta(t,z)|\,dz\left\|\overrightarrow{\mathbf{v}}(t)\right\| \\ &\leq \frac{1}{\delta}\|\overrightarrow{\mathbf{f}}(t)\| + \|\overrightarrow{\mathbf{v}}(0)\| + \|\overrightarrow{\mathbf{v}}(1)\| + \delta\left\|\overrightarrow{\mathbf{v}}(t)\right\|,\end{aligned}$$

which gives

$$\overrightarrow{\mathbf{v}}(t) \leq \frac{\left[\frac{1}{\delta}\|\overrightarrow{\mathbf{f}}(t)\| + \|\overrightarrow{\mathbf{v}}(0)\| + \|\overrightarrow{\mathbf{v}}(1)\|\right]}{1-\delta}.$$

Set $C_3 = \max\limits_{t\in[0,1]}\left\{\frac{\frac{1}{\delta}\|\overrightarrow{\mathbf{f}}(t)\| + \|\overrightarrow{\mathbf{v}}(0)\| + \|\overrightarrow{\mathbf{v}}(1)\|}{1-\delta}\right\}$, then $\overrightarrow{\mathbf{v}}(t) \leq C_3$.

Now the left singular component $\overrightarrow{\mathbf{w}}_L(t)$ is the solution of

$$\mathfrak{L}_{\varepsilon_1,\varepsilon_2}\overrightarrow{\mathbf{w}}_L(t) := \begin{pmatrix} -\varepsilon_1\frac{d^2}{dt^2} & 0 \\ 0 & -\varepsilon_2\frac{d^2}{dt^2}\end{pmatrix}\overrightarrow{\mathbf{w}}_L(t) + \mathbb{A}(t)\overrightarrow{\mathbf{w}}_L(t) = 0,$$

where

$$\overrightarrow{\mathbf{w}}_L(0) = (\overrightarrow{\mathbf{u}}(0) - \overrightarrow{\mathbf{v}}(0)), \quad \overrightarrow{\mathbf{w}}_L(1) = \overrightarrow{0},$$

and $\overrightarrow{\mathbf{w}}_L(t) = (w_1, w_2)^T$. Then

$$\begin{cases} |w_1(t)| \leq Ce^{-t\sqrt{\delta/\varepsilon_2}}, & \\ |w_2(t)| \leq Ce^{-t\sqrt{\delta/\varepsilon_2}}, & \\ |w_1^{(p)}(t)| \leq C\left(\varepsilon_1^{-p/2}e^{-t\sqrt{\delta/\varepsilon_1}} + \varepsilon_2^{-p/2}e^{-t\sqrt{\delta/\varepsilon_2}}\right), & \text{for } p = 1,2,3,4, \\ |w_2^{(p)}(t)| \leq C\varepsilon_2^{-p/2}e^{-t\sqrt{\delta/\varepsilon_2}}, & \text{for } p = 1,2, \\ |w_2^{(p)}(t)| \leq C\varepsilon_2^{-1}\left(\varepsilon_1^{(2-p)/2}e^{-t\sqrt{\delta/\varepsilon_1}} + \varepsilon_2^{(2-p)/2}e^{-t\sqrt{\delta/\varepsilon_2}}\right), & \text{for } p = 3,4. \end{cases}$$

The proof of the above equation is similar to the proof in [5].

Next right singular component $\overrightarrow{\mathbf{w}}_R(t)$ is solution of equation

$$\mathfrak{L}_{\varepsilon_1,\varepsilon_2}\overrightarrow{\mathbf{w}}_R(t) := \begin{pmatrix} -\varepsilon_1\frac{d^2}{dt^2} & 0 \\ 0 & -\varepsilon_2\frac{d^2}{dt^2} \end{pmatrix}\overrightarrow{\mathbf{w}}_R(t) + \mathbb{A}(t)\overrightarrow{\mathbf{w}}_R(t) = 0,$$

where

$$\overrightarrow{\mathbf{w}}_R(0) = \overrightarrow{0} \quad \text{and} \quad \overrightarrow{\mathbf{w}}_R(1) = (\overrightarrow{\mathbf{u}}(1) - \overrightarrow{\mathbf{v}}(1)).$$

The boundaries that correspond to the right layer component $\overrightarrow{\mathbf{w}}_R(t)$ can be derived by substituting t with $(1-t)$ in the expression $\overrightarrow{\mathbf{w}}_L(t)$. These bounds prove the lemma. □

Lemma 3. *[23] For all integer p on a fixed mesh, we have*

$$\lim_{\varepsilon\to 0}\max_{1\leq i\leq N-1}\left(\frac{e^{-\frac{C}{\sqrt{\varepsilon}}t_i}}{\varepsilon^{\frac{p}{2}}}\right) = 0 \textit{ and } \lim_{\varepsilon\to 0}\max_{1\leq i\leq N-1}\left(\frac{e^{-\frac{C}{\sqrt{\varepsilon}}(1-t_i)}}{\varepsilon^{\frac{p}{2}}}\right) = 0,$$

where $t_i = i(\Delta h)$.

3 Numerical discretization

On the interval $[0,1]$, the domain is divided into a uniform mesh with step size $\Delta h := \frac{1}{N}$, where N is the number of subintervals, and the mesh points are given by $t_i = i(\Delta h)$. The corresponding fitted difference operator for equation (1) is given by:

$$\mathfrak{L}^{(\Delta h)}_{\varepsilon_1,\varepsilon_2}\overrightarrow{\mathbf{U}}_i := \mathfrak{L}^{(\Delta h)}_1\overrightarrow{\mathbf{U}}_i + \mathfrak{L}^{(\Delta h)}_2\overrightarrow{\mathbf{U}}_i = \overrightarrow{\mathbf{f}}(t_i). \tag{3}$$

Using Mickens theory [20] for constructing NSFD schemes, a suitable nontraditional discretization is applied to the uniform step length. Accordingly, the discrete formulation of the operator $\mathfrak{L}_1$ is given by

$$\mathfrak{L}^{(\Delta h)}_1\overrightarrow{\mathbf{U}}_i = \begin{pmatrix} -\varepsilon_1\delta_1^2 & 0 \\ 0 & -\varepsilon_2\delta_2^2 \end{pmatrix}\overrightarrow{\mathbf{U}}_i + \mathbb{A}(t_i)\overrightarrow{\mathbf{U}}_i, \quad \text{for } i = 1,\ldots,N-1, \tag{4}$$

with boundary conditions

$$\overrightarrow{\mathbf{U}}_0 = \overrightarrow{\mathbf{u}}(0),\ \overrightarrow{\mathbf{U}}_N = \overrightarrow{\mathbf{u}}(1),$$

where $\delta_1^2 = \frac{U_{1,i-1}-2U_{1,i}+U_{1,i+1}}{\phi_i^2}$ and $\delta_2^2 = \frac{U_{2,i-1}-2U_{2,i}+U_{2,i+1}}{\psi_i^2}$ are the discrete approximations for NSFD scheme. Here $\phi_i^2 = \frac{2}{\rho_i}\sinh\left(\frac{\rho_i(\Delta h)}{2}\right)$, $\psi_i^2 = \frac{2}{\theta_i}\sinh\left(\frac{\theta_i(\Delta h)}{2}\right)$, with $\rho_i = \sqrt{\frac{a_{11,i}}{\varepsilon_1}}$ and $\theta_i = \sqrt{\frac{a_{22,i}}{\varepsilon_2}}$.

Therefore equation (4) is transformed in the following form:

$$\mathfrak{L}^{(\Delta h)}_1 = \begin{cases} -\varepsilon_1\dfrac{U_{1,i-1}-2U_{1,i}+U_{1,i+1}}{\phi_i^2} + a_{11,i}U_{1,i} + a_{12,i}U_{2,i}, \\ -\varepsilon_2\dfrac{U_{2,i-1}-2U_{2,i}+U_{2,i+1}}{\psi_i^2} + a_{22,i}U_{2,i} + a_{21,i}U_{1,i}, \quad i = 1,\ldots,N-1. \end{cases}$$

Now by applying the composite trapezoidal rule for the integral operator in $\mathfrak{L}_2$ by [17], we get

$$\mathfrak{L}_2^{(\Delta h)} = \begin{cases} \lambda \sum_{l=0}^{N} \tau_l(\Delta h)\,\Theta(t_i,z_l)\,U_{1,l} \\ \lambda \sum_{l=0}^{N} \tau_l(\Delta h)\,\Theta(t_i,z_l)\,U_{2,l}, \quad i=1,\ldots,N-1, \end{cases}$$

where, $\tau_l = \begin{cases} \frac{1}{2} & \text{for } l=0 \text{ and } N, \\ 1 & \text{for } l=1,2,\ldots,N-1. \end{cases}$

Then using equation (3) implies

$$\mathfrak{L}^{(\Delta h)}\overrightarrow{\mathbf{U}}_i := \begin{cases} -\varepsilon_1 \frac{U_{1,i-1}-2U_{1,i}+U_{1,i+1}}{\phi_i^2} + a_{11,i}U_{1,i} + a_{12,i}U_{2,i} + \lambda \sum_{l=0}^{N} \tau_l(\Delta h)\,\Theta(t_i,z_l)\,U_{1,l} = f_1(t_i), \\ -\varepsilon_2 \frac{U_{2,i-1}-2U_{2,i}+U_{2,i+1}}{\psi_i^2} + a_{22,i}U_{2,i} + a_{21,i}U_{1,i} + \lambda \sum_{l=0}^{N} \tau_l(\Delta h)\,\Theta(t_i,z_l)\,U_{2,l} = f_2(t_i), \end{cases}$$

with $U_{1,0}=u_1(0)$, $U_{2,0}=u_2(0)$, $U_{1,N}=u_1(1)$, $U_{2,N}=u_2(1)$.

4 Error analysis

The error bound calculations are separated into $\mathfrak{L}_1$ and $\mathfrak{L}_2$ operators. In $\mathfrak{L}_1$ operator the local truncation error of the first component solution is

$$\mathscr{L}_1^{(\Delta h)}(u_{1,i}-U_{1,i}) = -\varepsilon_1 u''_{1,i} + \varepsilon_1 \frac{U_{1,i-1}-2U_{1,i}+U_{1,i+1}}{\phi_i^2}.$$

Applying the Taylor expansions for ϕ_i and $U_{1,i\pm1}$, gives

$$\mathscr{L}_1^{(\Delta h)}(u_{1,i}-U_{1,i}) = -\varepsilon_1\Bigg[u''_{1,i} - \left((\Delta h)^2 u''_{1,i} + \frac{(\Delta h)^4}{24}(u_1^{(iv)}(\eta_1)+u_1^{(iv)}(\eta_2))\right) \times \left(\frac{1}{(\Delta h)^2} - \frac{\rho_i^2}{12} + \frac{\rho_i^4(\Delta h)^2}{240}\right)\Bigg],$$

where $\eta_1 \in (t_{i-1},t_i)$ and $\eta_2 \in (t_i,t_{i+1})$. By using the value of ρ_i, the following bound is derived:

$$\left|\mathscr{L}_1^{(\Delta h)}(u_{1,i}-U_{1,i})\right| \leq \frac{\varepsilon_1(\Delta h)^2}{12}|u_1^{(iv)}(\eta_i)| + \frac{a_{11,i}(\Delta h)^2}{12}|u''_{1,i}| + \frac{a_{11,i}(\Delta h)^4}{144}|u_1^{(iv)}(\eta_i)| + \frac{a_{11,i}^2(\Delta h)^4}{240}\left|\frac{u''_{1,i}}{\varepsilon_1}\right| + \frac{a_{11,i}^2(\Delta h)^6}{2880}\left|\frac{u_1^{(iv)}(\eta_i)}{\varepsilon_1}\right|,$$

where $\eta_i \in (t_{i-1},t_{i+1})$. By applying the Lemmas 2 and 3, shows immediately that $|u''_1| \leq C_1$ and $|u_1^{(iv)}(\eta_i)| \leq C_1$. Also, we note that

$$\left|\frac{u''_{1,i}}{\varepsilon_1}\right| \leq C_1\left[\frac{\varepsilon_1 + e^{-t_i\sqrt{\frac{\delta}{\varepsilon_1}}} + e^{-(1-t_i)\sqrt{\frac{\delta}{\varepsilon_1}}}}{\varepsilon_1^2} + \frac{e^{-t_i\sqrt{\frac{\delta}{\varepsilon_2}}} + e^{-(1-t_i)\sqrt{\frac{\delta}{\varepsilon_2}}}}{\varepsilon_1\varepsilon_2}\right].$$

But, for all $s \in (0, t_i)$, we have

$$e^{-t_i\sqrt{\frac{\delta}{\varepsilon_1}}} < e^{-s\sqrt{\frac{\delta}{\varepsilon_1}}}.$$

When ε_1 approaches zero, $e^{-t_i\sqrt{\frac{\delta}{\varepsilon_1}}}$ will tend to zero faster than $e^{-s\sqrt{\frac{\delta}{\varepsilon_1}}}$, thus widening the gap between these two quantities. It follows that

$$\varepsilon_1 + e^{-t_i\sqrt{\frac{\delta}{\varepsilon_1}}} < e^{-s\sqrt{\frac{\delta}{\varepsilon_1}}}.$$

In this way, it follows that $\left|\frac{u''_{1,i}}{\varepsilon_1}\right| \leq C_1$. In a similar approach $\left|\frac{u^{(iv)}_{1,i}}{\varepsilon_1}\right| \leq C_1$. Then the inequality leads to

$$\left|\mathscr{L}_1^{(\Delta h)}(u_{1,i} - U_{1,i})\right| \leq C_1(\Delta h)^2. \tag{5}$$

Now, the local truncation error of the second component solution in $\mathfrak{L}_1$ operator is

$$\begin{aligned}\left|\mathscr{L}_2^{(\Delta h)}(u_{2,i} - U_{2,i})\right| \leq & \frac{\varepsilon_2(\Delta h)^2}{12}|u_2^{(iv)}(\eta_i)| + \frac{a_{22,i}(\Delta h)^2}{12}|u''_{2,i}| + \frac{a_{22,i}(\Delta h)^4}{144}|u_2^{(iv)}(\eta_i)| \\ & + \frac{a^2_{22,i}(\Delta h)^4}{240}\left|\frac{u''_{2,i}}{\varepsilon_2}\right| + \frac{a^2_{22,i}(\Delta h)^6}{2880}\left|\frac{u_2^{(iv)}(\eta_i)}{\varepsilon_2}\right|,\end{aligned}$$

where $\eta_i \in (t_{i-1}, t_{i+1})$. Similar arguments gives

$$\left|\mathscr{L}_2^{(\Delta h)}(u_{2,i} - U_{2,i})\right| \leq C_1(\Delta h)^2. \tag{6}$$

By equations (5) and (6), it follows that

$$\left|\mathfrak{L}_1^{(\Delta h)}(\vec{\mathbf{u}} - \vec{\mathbf{U}})_i\right| \leq C_1(\Delta h)^2, \tag{7}$$

where C_1 is independent of $\varepsilon_1, \varepsilon_2$ and Δh. Next, the error estimation of the integral operator $\mathfrak{L}_2$ is also splitted into two components. The first component error bound is

$$\begin{aligned}\mathscr{L}_3^{(\Delta h)}(u_{1,i} - U_{1,i}) &= \lambda\int_0^1 \Theta(t_i, z)u_1(z)\,dz - \lambda\sum_{l=0}^{N}\tau_l(\Delta h)\,\Theta(t_i, z_l)\,U_{1,l}, \\ &= \lambda(\frac{-1}{12})(\Delta h)^2\left|\frac{\partial^2}{\partial\xi^2}\Theta(t_i,\xi)u_1(\xi)\right|,\ \xi \in [0,1].\end{aligned}$$

By applying the bound $|\lambda| \leq \dfrac{\delta}{\max\limits_{0\leq t\leq 1}\int_0^1|\Theta(t,\xi)|d\xi}$, we have

$$\begin{aligned}\left|\mathscr{L}_3^{(\Delta h)}(u_{1,i} - U_{1,i})\right| &\leq \frac{1}{12}|\lambda|(\Delta h)^2\max_{0\leq t_i,\xi\leq 1}\left|\frac{\partial^2}{\partial\xi^2}[\Theta(t_i,\xi)u_1(\xi)]\right|, \\ &\leq C_2(\Delta h)^2. \end{aligned}\tag{8}$$

Now, the error bound of the second component of the integral part is

$$\begin{aligned}\mathscr{L}_4^{(\Delta h)}(u_{2,i}-U_{2,i}) &= \lambda\int_0^1 \Theta(t_i,z)u_2(z)\,dz-\lambda\sum_{l=0}^{N}\tau_l(\Delta h)\Theta(t_i,z_l)U_{2,l},\\ &= \lambda(\frac{-1}{12})(\Delta h)^2\max_{0\le t_i,\xi\le 1}\left|\frac{\partial^2}{\partial\xi^2}\Theta(t_i,\xi)u_2(\xi)\right|,\ \xi\in[0,1].\end{aligned}$$

By applying the bound $|\lambda|\le\dfrac{\delta}{\max\limits_{0\le t\le 1}\int_0^1|\Theta(t,z)|dz}$, we have

$$\begin{aligned}\left|\mathscr{L}_4^{(\Delta h)}(u_{2,i}-U_{2,i})\right| &\le \frac{1}{12}|\lambda|(\Delta h)^2\max_{0\le t_i,\xi\le 1}\left|\frac{\partial^2}{\partial\xi^2}[\Theta(t_i,\xi)u_2(\xi)]\right|\\ &\le C_2(\Delta h)^2. \end{aligned}\tag{9}$$

By equations (8) and (9), it follows that

$$\left|\mathfrak{L}_2^{(\Delta h)}(\vec{\mathbf{u}}-\vec{\mathbf{U}})_i\right|\le C_2(\Delta h)^2,\tag{10}$$

where C_2 is independent of $\varepsilon_1,\varepsilon_2$ and Δh.

Theorem 1. *Let $\vec{\mathbf{u}}_i$ and $\vec{\mathbf{U}}_i$ be the continuous and numerical solution of equations (1) and (3), respectively. Then*

$$\sup_{0<\varepsilon_1\le\varepsilon_2\le 1}\max_{0\le i\le N}\left|\vec{\mathbf{u}}(t_i)-\vec{\mathbf{U}}_i\right|\le C(\Delta h)^2,$$

where C is independent of $\varepsilon_1,\varepsilon_2$ and Δh.

Proof. Let

$$\begin{aligned}\left|\mathfrak{L}_{\varepsilon_1,\varepsilon_2}\vec{\mathbf{u}}(t_i)-\mathfrak{L}_{\varepsilon_1,\varepsilon_2}^{(\Delta h)}\vec{\mathbf{U}}_i\right| &= \left|\left(\mathfrak{L}_1\vec{\mathbf{u}}(t_i)+\mathfrak{L}_2\vec{\mathbf{u}}(t_i)\right)-\left(\mathfrak{L}_1^{(\Delta h)}\vec{\mathbf{U}}_i+\mathfrak{L}_2^{(\Delta h)}\vec{\mathbf{U}}_i\right)\right|\\ &\le \left|\mathfrak{L}_1\vec{\mathbf{u}}(t_i)-\mathfrak{L}_1^{(\Delta h)}\vec{\mathbf{U}}_i\right|+\left|\mathfrak{L}_2\vec{\mathbf{u}}(t_i)-\mathfrak{L}_2^{(\Delta h)}\vec{\mathbf{U}}_i\right|.\end{aligned}$$

Applying the equations (7) and (10) gives

$$\begin{aligned}\left|\mathfrak{L}_{\varepsilon_1,\varepsilon_2}\vec{\mathbf{u}}(t_i)-\mathfrak{L}_{\varepsilon_1,\varepsilon_2}^{(\Delta h)}\vec{\mathbf{U}}_i\right| &\le C_1(\Delta h)^2+C_2(\Delta h)^2\\ &\le C(\Delta h)^2.\end{aligned}$$

$\square$

5 Numerical results

According to the theoretical analysis, the developed method exhibits a uniform convergence rate of order two, regardless of the perturbation parameters ε_1 and ε_2. Numerical computations were performed to evaluate the efficiency of the NSFD and composite trapezoidal rule methodology, utilizing the given instance.

Example 1. Consider the system of SPFIDE in the form of equation (1)

$$\begin{cases} -\varepsilon_1 u_1''(t) + 2(t+1)^2 u_1(t) - (1+t^3)u_2(t) + \frac{1}{2}\int\limits_0^1 t\, u_1(z)\, dz = 2\exp(t), \\ -\varepsilon_2 u_2''(t) - 2\cos\left(\frac{t\pi}{4}\right) u_1(t) + 2.2\exp(t-1)u_2(t) + \frac{1}{2}\int\limits_0^1 t\, u_2(z)\, dz = 1+10t, \end{cases}$$

with the boundary conditions $\begin{pmatrix} u_1(0) \\ u_2(0) \end{pmatrix} = \begin{pmatrix} 0 \\ 0 \end{pmatrix}, \quad \begin{pmatrix} u_1(1) \\ u_2(1) \end{pmatrix} = \begin{pmatrix} 0 \\ 0 \end{pmatrix}.$

Example 1 does not have an exact solution. Consequently, an error estimate is followed by a double mesh error analysis. The errors obtained by

$$\mathrm{E}_1^N = \max_{0\le i\le N} \left|U_1^N - U_1^{2N}\right|,$$
$$\mathrm{E}_2^N = \max_{0\le i\le N} \left|U_2^N - U_2^{2N}\right|,$$

where E_1^N and E_2^N are the maximum absolute errors of the first and second components of the solutions $u_1(t)$ and $u_2(t)$, respectively.

Then the convergence rate is computed using the following formula:

$$\mathfrak{R}_k := \log_2\left(\frac{\mathrm{E}_k^N}{\mathrm{E}_k^{2N}}\right), \quad k = 1,2.$$

The following example illustrates the m-system model; theoretical details are provided in the appendix.

Example 2. Consider the system of SPFIDE in the form of equation (A.1)

$$\begin{cases} -\varepsilon_1 u_1''(t) + (t+7)^2 u_1(t) - (1+t^2)u_2(t) - 2u_3(t) + \frac{1}{2}\int\limits_0^1 (t+z)u_1(z)\, dz = t^2+3, \\ -\varepsilon_2 u_2''(t) - 1u_1(t) + (t^2+6)u_2(t) - (2+t)u_3(t) + \frac{1}{2}\int\limits_0^1 (t+z)u_2(z)\, dz = t+1, \\ -\varepsilon_2 u_3''(t) - 2u_1(t) - (e^t+1)u_2(t) + (t^3+5)u_3(t) + \frac{1}{2}\int\limits_0^1 (t+z)u_3(z)\, dz = 2t^3+5, \end{cases}$$

with boundary conditions

$$\begin{pmatrix} u_1(0) \\ u_2(0) \\ u_3(0) \end{pmatrix} = \begin{pmatrix} 0 \\ 0 \\ 0 \end{pmatrix}, \quad \begin{pmatrix} u_1(1) \\ u_2(1) \\ u_3(1) \end{pmatrix} = \begin{pmatrix} 0 \\ 0 \\ 0 \end{pmatrix}.$$

In this Example 2 the double mesh principle is applied to estimate the error bound and convergence order. The uniform errors for each N is

$$\mathfrak{E}_k^N = \max_{0\leq\varepsilon_1\leq\varepsilon_2\leq\varepsilon_3\leq 1}\left(\max_{0\leq i\leq N}\left|U_k^N - U_k^{2N}\right|\right), \quad \text{for } k = 1,2,3.$$

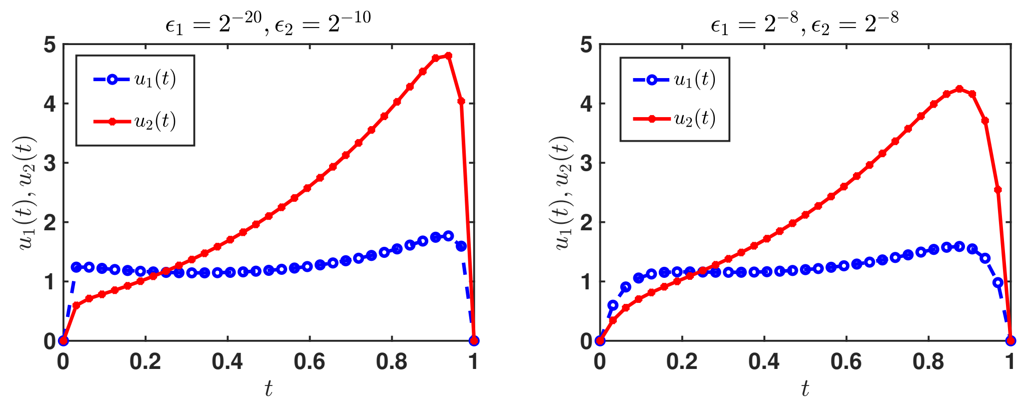

Figure 1: Solution plots of Example 1 for $N = 64$.

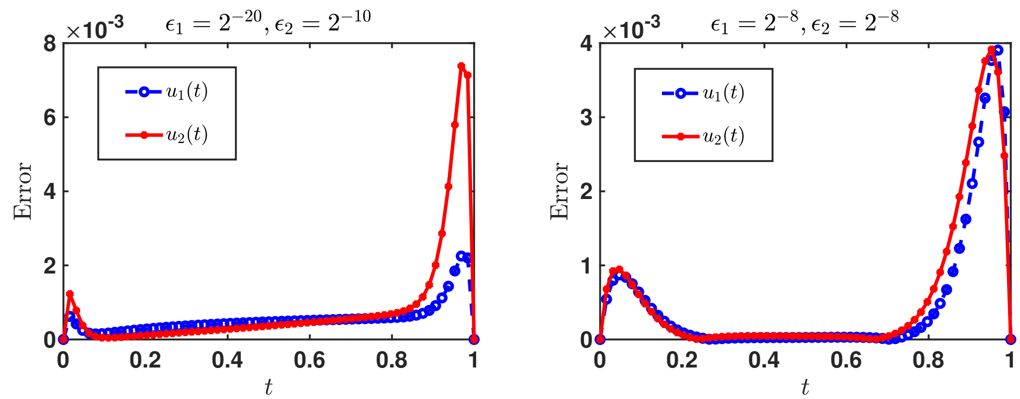

Figure 2: Error plots of Example 1 for $N = 64$.

The computational solution plots of $u_1(t)$ and $u_2(t)$, for different values of ε_1 and ε_2 of Example 1, are shown in Figure 1. The corresponding error plots with $N = 64$ mesh points are presented in Figure 2. Table 1 and Table 2 provide the maximum absolute errors of U_1, U_2, and their rates of convergence with various values of ε_2 and a fixed value of $\varepsilon_1 = 2^{-14}$, respectively. Likewise, Tables 3 and 4 present the maximum absolute errors of U_1, U_2, and convergence rates when $\varepsilon_1 = \varepsilon_2$. All tables indicate that the rate of convergences is almost two. Figures 3(a) and 3(b) expose the numerical convergence rates on the log-log scale to provide a graphical representation. Further, the solution plots of Example 2 are shown in Figure 4, the corresponding error plots are displayed in Figure 5, and the uniform errors and convergence rates of Example 2 are presented in Tables 5, 6, and 7, respectively.

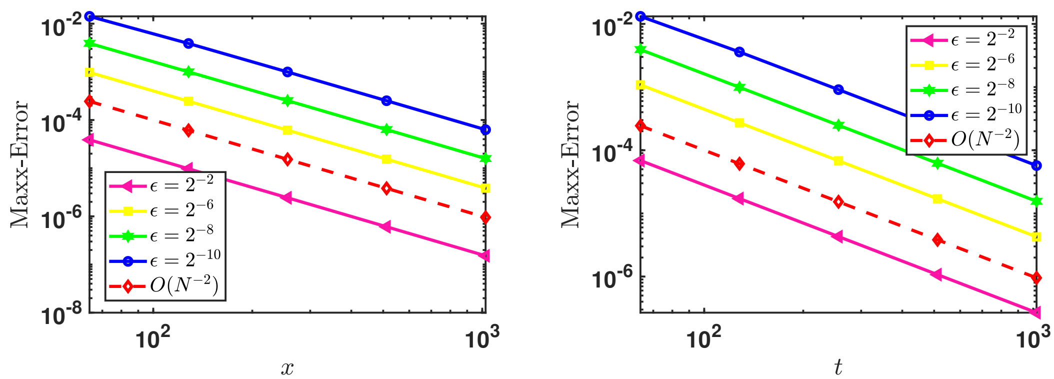

(a) $u_1(t)$ of Example 1 (b) $u_2(t)$ of Example 1

Figure 3: Log-log plot with corresponding values of $\varepsilon = \varepsilon_1 = \varepsilon_2$.

Table 1: E_1^N of U_1 and $\mathfrak{R}_1$ of Example 1.

	Number of mesh points N and $\varepsilon_1 = 2^{-14}$				
$\varepsilon_2 \downarrow$	$N = 64$	$N = 128$	$N = 256$	$N = 512$	$N = 1024$
2^{-2}	6.9540e-4	4.4144e-4	1.2289e-4	3.3310e-5	8.3905e-6
	0.6556	1.8449	1.8833	1.9891	1.9972
2^{-4}	9.3905e-4	5.0906e-4	1.4105e-4	3.7186e-5	9.3630e-6
	0.8834	1.8516	1.9234	1.9897	1.9955
2^{-6}	1.7110e-3	7.2914e-4	1.9987e-4	5.1201e-5	1.2880e-5
	1.2306	1.8671	1.9648	1.9911	1.9978
2^{-8}	3.9101e-3	1.5224e-3	5.3339e-4	1.4493e-4	3.7062e-5
	1.3609	1.5131	1.8798	1.9674	1.9923
2^{-10}	8.4760e-3	5.1526e-3	1.7630e-3	4.7961e-4	1.2251e-4
	0.7181	1.5473	1.8781	1.9690	1.9922
2^{-12}	1.7121e-2	1.5253e-2	5.1981e-3	1.4650e-3	3.7426e-4
	0.1667	1.5530	1.8271	1.9688	1.9922

6 Conculsion

The present article analyzes the numerical solution of a system of second-order singularly perturbed Fredholm integro-differential equations achieving an approximate order of $(\Delta h)^2$. The suggested approach employs a non-standard finite difference scheme for the differential terms and applies the composite trapezoidal rule to the integral terms. The theoretical evaluation of the suggested approach indicates that it obtains a convergence order of $(\Delta h)^2$. A computational example validates the efficacy of the theoretical findings. The novel technique for numerical solutions involves solving the system of second-order singularly perturbed Fredholm integro-differential equations using a fitted operator method. The approach is also applicable to the m-system of singularly perturbed Fredholm integro-differential equations.

Table 2: E_2^N of U_2 and $\mathfrak{R}_2$ of Example 1.

	Number of mesh points N and $\varepsilon_1 = 2^{-14}$				
$\varepsilon_2 \downarrow$	$N = 64$	$N = 128$	$N = 256$	$N = 512$	$N = 1024$
2^{-2}	1.3696e-4	4.2515e-5	1.1588e-5	2.9708e-6	7.4759e-7
	1.6877	1.8754	1.9637	1.9905	1.9980
2^{-4}	3.4988e-4	1.0874e-4	3.0109e-5	7.7640e-6	1.9569e-6
	1.6859	1.8527	1.9553	1.9882	1.9970
2^{-6}	9.8392e-4	3.2849e-4	9.1940e-5	2.3932e-5	6.0472e-6
	1.5827	1.8371	1.9417	1.9846	1.9961
2^{-8}	3.0777e-3	1.0646e-3	3.1125e-4	8.1723e-5	2.0696e-5
	1.5316	1.7742	1.9292	1.9814	1.9953
2^{-10}	9.6535e-3	3.7088e-3	1.1155e-3	2.9427e-4	7.4603e-5
	1.3801	1.7333	1.9224	1.9798	1.9948
2^{-12}	2.9274e-2	1.2828e-2	3.8895e-3	1.0407e-3	2.6380e-4
	1.1903	1.7216	1.9020	1.9800	1.9947

Table 3: E_1^N of U_1 and $\mathfrak{R}_1$ of Example 1.

	Number of mesh points N and $\varepsilon_1 = \varepsilon_2$				
$\varepsilon_1 = \varepsilon_2$	$N = 64$	$N = 128$	$N = 256$	$N = 512$	$N = 1024$
2^{-2}	3.8842e-5	9.7131e-6	2.4284e-6	6.0700e-7	1.5144e-7
	1.9996	1.9999	2.0003	2.0030	2.0554
2^{-4}	2.1059e-4	5.2726e-5	1.3186e-5	3.2969e-6	8.2425e-7
	1.9979	1.9995	1.9999	2.0000	2.0001
2^{-6}	9.7418e-4	2.4572e-4	6.1517e-5	1.5390e-5	3.8479e-6
	1.9872	1.9979	1.9990	1.9999	2.0000
2^{-8}	3.9056e-3	9.9938e-4	2.5267e-4	6.3257e-5	1.5820e-5
	1.9664	1.9838	1.9979	1.9995	1.9999
2^{-10}	1.4199e-2	3.8823e-3	9.9444e-4	2.5138e-4	6.2938e-5
	1.8708	1.9650	1.9840	1.9979	1.9995
2^{-12}	3.4014e-2	1.4058e-2	3.8494e-3	9.8576e-4	2.4928e-4
	1.2747	1.8687	1.9653	1.9835	1.9979

Appendix

Equation (1) extended to $m-$systems of equation

$$\begin{cases} \mathbb{L}\overrightarrow{\mathbf{u}}(t) := \mathbb{L}_1\overrightarrow{\mathbf{u}}(t) + \mathbb{L}_2\overrightarrow{\mathbf{u}}(t) = \overrightarrow{\mathbf{f}}(t), \quad t \in (0,1), \\ \overrightarrow{\mathbf{u}}(0) = B_0, \quad \overrightarrow{\mathbf{u}}(1) = B_1, \end{cases} \tag{A.1}$$

Table 4: E_2^N of U_2 and $\mathfrak{R}_2$ of Example 1.

	Number of mesh points N and $\varepsilon_1 = \varepsilon_2$				
$\varepsilon_1 = \varepsilon_2$	$N = 64$	$N = 128$	$N = 256$	$N = 512$	$N = 1024$
2^{-2}	6.8619e-5	1.7157e-5	4.2893e-6	1.0723e-6	2.6808e-7
	1.9998	2.0000	2.0000	2.0000	2.0018
2^{-4}	2.8545e-4	7.1403e-5	1.7853e-5	4.4636e-6	1.1159e-6
	1.9992	1.9998	1.9999	2.0000	2.0000
2^{-6}	1.0842e-3	2.7181e-4	6.8058e-5	1.7017e-5	4.2545e-6
	1.9959	1.9978	1.9998	1.9999	2.0000
2^{-8}	3.9162e-3	9.9057e-4	2.4837e-4	6.2148e-5	1.5542e-5
	1.9831	1.9958	1.9987	1.9995	1.9999
2^{-10}	1.3159e-2	3.5921e-3	9.0960e-4	2.2824e-4	5.7140e-5
	1.8731	1.9815	1.9947	1.9980	1.9997
2^{-12}	3.9744e-2	1.2389e-2	3.3884e-3	8.5864e-4	2.1557e-4
	1.6816	1.8704	1.9805	1.9939	1.9982

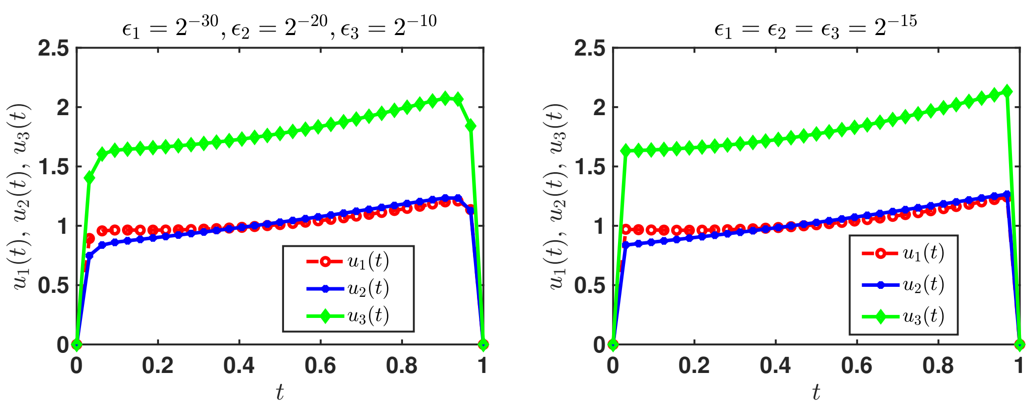

Figure 4: Solution plots of Example 2 for $N = 64$.

Table 5: Uniform errors and rate of convergences of U_1 for Example 2.

$(\varepsilon_1 \le \varepsilon_2 \le \varepsilon_3) \downarrow$	Number of mesh points N						
	N=64	N=128	N=256	N=512	N=1024	N=2048	N=4096
$\mathfrak{E}_1^N$	1.5103e-2 1.8799	4.1036e-3 1.9665	1.0500e-3 1.9935	2.6369e-4 1.9975	6.6037e-5 1.9997	1.6513e-5 1.9998	4.1287e-6 –

where, $\mathbb{L}_1 = -\mathfrak{Eps}(\overrightarrow{\mathbf{u}}(t))'' + \mathbb{A}(t)\overrightarrow{\mathbf{u}}(t)$, $\mathbb{L}_2 = \lambda \int\limits_0^1 \Theta(t,z)\overrightarrow{\mathbf{u}}(z)\,dz$, $\mathfrak{Eps} = \operatorname{diag}(\varepsilon_1, \varepsilon_2, \ldots, \varepsilon_m)$, $0 < \varepsilon_i \le \varepsilon_j \ll 1$, $1 \le i \le j \le m$, $\mathbb{A}(t) = (a_{ij}(t))_{m\times m}$, $\overrightarrow{\mathbf{f}}(t) = (f_1(t), f_2(t), \ldots, f_m(t))^T$,

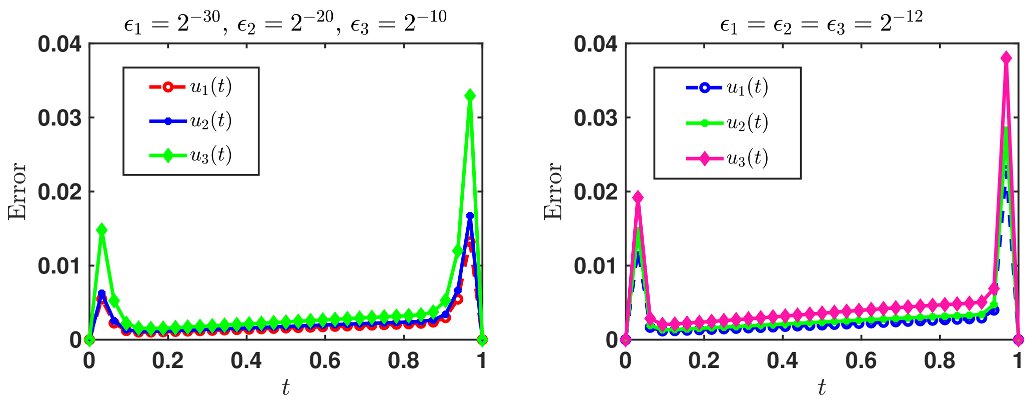

Figure 5: Error plots of Example 2 for $N = 64$.

Table 6: Uniform errors and rate of convergences of U_2 for Example 2.

$(\varepsilon_1 \leq \varepsilon_2 \leq \varepsilon_3) \downarrow$	Number of mesh points N						
	N=64	N=128	N=256	N=512	N=1024	N=2048	N=4096
$\mathfrak{E}_2^N$	1.8358e-2	4.9513e-3	1.2738e-3	3.1974e-4	8.0018e-5	2.0015e-5	5.0041e-6
	1.8905	1.9587	1.9942	1.9985	1.9992	1.9999	–

Table 7: Uniform errors and rate of convergences of U_3 for Example 2.

$(\varepsilon_1 \leq \varepsilon_2 \leq \varepsilon_3) \downarrow$	Number of mesh points N						
	N=64	N=128	N=256	N=512	N=1024	N=2048	N=4096
$\mathfrak{E}_3^N$	2.0617e-2	5.7756e-3	1.4623e-3	3.6671e-4	9.1749e-5	2.2942e-5	5.7357e-6
	1.8358	1.9817	1.9955	1.9989	1.9997	1.9999	–

$\overrightarrow{\mathbf{u}}(t) = (u_1(t), u_2(t), \cdots, u_m(t))^T$ and B_0, B_1 are constants. Also,

$$
\begin{aligned}
&a_{ii}(t) > |a_{ij}(t)|,\, j \neq i, \quad t \in \bar{\Omega},\\
&a_{ij}(t) \leq 0,\, i \neq j, \quad t \in \bar{\Omega},\\
&\min_i \{\sum_{j=1}^{m} a_{ij}(t) \geq \delta > 0.
\end{aligned}
$$

The solution bound and derivation bound of the equation (A.1) can be found in the following lemma.

Lemma 4. *Let the solution $\overrightarrow{\mathbf{u}}(t)$ be decomposed into regular component $\overrightarrow{\mathbf{v}}(t)$ and singular component $\overrightarrow{\mathbf{w}}(t)$. If $\frac{\partial^r \Theta(t,z)}{\partial t^r} \in C([0,1] \times [0,1])$ for $r = 0,1,2,3,4$ and $f_i(t)$, $a_{ij}(t)$ are $C^2[0,1]$ for $i, j = 1,2,\ldots,m$.*

Then there exists a C is a independent constant of $\varepsilon_i\,(i = 1,2,\dots,m)$ *such that*

$$\|v_i^{(r)}(t)\| \le C\left(1+\varepsilon_i^{\frac{2-r}{2}}\right), \quad \textit{for } r = 0,1,2,3,4,$$

$$|w_i^{(r)}(t)| \le C\sum_{n=i}^{m} \varepsilon_n^{-r/2}\mathscr{D}_{\varepsilon_n}(t), \quad \textit{for } r = 0,1,2,$$

$$|w_i^{(r)}(t)| \le C\varepsilon_i^{(2-r)/2}\sum_{n=i}^{m} \varepsilon_n^{-1}\mathscr{D}_{\varepsilon_n}(t), \quad \textit{for } r = 3,4,$$

where $\mathscr{D}_{\varepsilon_n}(t) = \exp\left(-t\sqrt{\frac{\delta}{\varepsilon_n}}\right) + \exp\left(-(1-t)\sqrt{\frac{\delta}{\varepsilon_n}}\right)$.

Proof. It follows using Lemma 2 and proof method of Theorem 2.4 in [19]. □

The error estimates following the next lemma.

Lemma 5. *Let* $\overrightarrow{\mathbf{u}}_i$ *and* $\overrightarrow{\mathbf{U}}_i$ *be the continuous and numerical solution of the equations (A.1). Then*

$$\sup_{0<\varepsilon_k\le\varepsilon_j\le 1}\ \max_{0\le i\le N}\left|\overrightarrow{\mathbf{u}}(t_i) - \overrightarrow{\mathbf{U}}_i\right| \le C(\Delta h)^2,$$

where C is independent of $\varepsilon_k, \varepsilon_j\,(k,j = 1,2,\dots,m)$.

Proof. The proof is similar to the proof of Theorem 1. □

References

[1] I. Amirali, M.E. Durmaz, G.M. Amiraliyev, *A monotone second-order numerical method for Fredholm integro-differential equation*, Mediterr. J. Math. **21** (2024) 198.

[2] M. Banerjee, M. Kuznetsov, O. Udovenko, V. Volpert, *Nonlocal reaction-diffusion equations in biomedical applications*, Acta Biotheor. **70** (2022) 12.

[3] J. Biazar, E. Babolian, R. Islam, *Solution of a system of Volterra integral equations of the first kind by Adomian method*, Appl. Math. Comput. **139** (2003) 249–258.

[4] E. Cimen, M. Cakir, *A uniform numerical method for solving singularly perturbed Fredholm integro-differential problem*, Comput. Appl. Math. **40** (2021) 42.

[5] C. Clavero, J.L. Gracia, F.J. Lisbona, *An almost third order finite difference scheme for singularly perturbed reaction-diffusion systems*, J. Comput. Appl. Math. **234** (2010) 2501–2515.

[6] L.A. Dawood, A. Hamoud, N.M. Mohammed, *Laplace discrete decomposition method for solving nonlinear Volterra-Fredholm integro-differential equations*, J. Math. Comput. Sci. **21** (2020) 158–163.

[7] P. Deepika, A. Das, *A robust numerical scheme via grid equidistribution for singularly perturbed delay partial differential equations arising in control theory*, Int. J. Appl. Comput. Math. **10** (2024) 72.

[8] M.E. Durmaz, G.M. Amiraliyev, *A robust numerical method for a singularly perturbed Fredholm integro-differential equation*, Mediterr. J. Math. **18** (2021) 24.

[9] S. Elango, A. Tamilselvan, *Singularly perturbed delay differential equations of convection-diffusion type with integral boundary condition*, J. Appl. Math. Comput. **59** (2019) 701–722.

[10] S. Elango, *Second order singularly perturbed delay differential equations with nonlocal boundary condition*, J. Comput. Appl. Math. **417** (2023) 114498.

[11] S. Elango, L. Govindarao, M. Awadalla, H. Zaway, *Efficient Numerical Methods for Reaction–Diffusion Problems Governed by Singularly Perturbed Fredholm Integro-Differential Equations*, Mathematics **13** (2025) 1511.

[12] S. Elango, L. Govindarao, J. Mohapatra, R. Vadivel, N.T. Hu, *Numerical analysis for second order differential equation of reaction-diffusion problems in viscoelasticity*, Alexandria Eng. J. **92** (2024) 92–101.

[13] S. Elango, L. Govindarao, R. Vadivel, *A comparative study on numerical methods for Fredholm integro-differential equations of convection-diffusion problem with integral boundary conditions*, Appl. Numer. Math. **207** (2025) 323–338.

[14] L. Govindarao, J. Mohapatra, A. Das, *A fourth-order numerical scheme for singularly perturbed delay parabolic problem arising in population dynamics*, J. Appl. Math. Comput. **63** (2020) 171–195.

[15] L. Govindarao, H. Ramos, S. Elango, *Numerical scheme for singularly perturbed Fredholm integro-differential equations with non-local boundary conditions*, Comput. Appl. Math. **43** (2024) 126.

[16] L. Govindarao, E. Sekar, *B-spline method for second order RLC closed series circuit with small inductance value*, J. Phys.: Conf. Ser. **2646** (2023) 012039.

[17] R. Kress, *Numerical Analysis*, Springer, New York, 1998.

[18] C.G. Lange, D.R. Smith, *Singular perturbation analysis of integral equations*, Stud. Appl. Math. **90** (1993) 1–74.

[19] T. Linß, N. Madden, *Layer-adapted meshes for a linear system of coupled singularly perturbed reaction-diffusion problems*, IMA J. Numer. Anal. **29** (2009) 109–125.

[20] R.E. Mickens, *Nonstandard finite difference models of differential equations*, World Scientific, Singapore, 1994.

[21] J.J.H. Miller, E. O'Riordan, G.I. Shishkin, *Fitted Numerical Methods for Singular Perturbation Problems*, World Scientific, Singapore, 1996.

[22] J. Mohapatra, L. Govindarao, S. Priyadarshana, *A splitting based higher-order numerical scheme for 2D time-dependent singularly perturbed reaction-diffusion problems*, J. Supercomput. **81** (2025) 203.

[23] J.B. Munyakazi, K.C. Patidar, *An efficient numerical method for a system of singularly perturbed reaction-diffusion equations*, Neural Parallel Sci. Comput. **20** (2012) 173.

[24] NT. Hu, E. Sekar, CS. Chen, M. Manigandan, *Computational methods for singularly perturbed differential equations with the advanced argument of convection-diffusion type*, AIMS Math. **9** (2024) 22547–22564.

[25] A. Panda, J. Mohapatra, *On the convergence analysis of efficient numerical schemes for singularly perturbed second order Volterra integro-differential equations*, J. Appl. Math. Comput. **69** (2023) 3509–3532.

[26] A. Panda, J. Mohapatra, I. Amirali, M.E. Durmaz, G.M. Amiraliyev, *A numerical technique for solving nonlinear singularly perturbed Fredholm integro-differential equations*, Math. Comput. Simul. **220** (2024) 618–629.

[27] S. Priyadarshana, A. Padhan, J. Mohapatra, *Adaptive grid based moving mesh algorithms for singularly perturbed second-order Volterra integro differential equations*, Quaest. Math. (2025) 1–22 https://doi.org/10.2989/16073606.2025.2462939.

[28] S. Priyadarshana, J. Mohapatra, *An efficient computational technique for time dependent semilinear parabolic problems involving two small parameters*, J. Appl. Math. Comput. **69** (2023) 3721–3754.

[29] S. Priyadarshana, J. Mohapatra, H. Ramos, *Robust numerical schemes for time delayed singularly perturbed parabolic problems with discontinuous convection and source terms*, Calcolo **61** (2024) 1.

[30] S. Priyadarshana, J. Mohapatra, *An efficient fractional step numerical algorithm for time-delayed singularly perturbed 2D convection-diffusion-reaction problem with two small parameters*, Numer. Algor. **97** (2024) 687–726.

[31] S. Priyadarshana, *Monotone hybrid numerical method for singularly perturbed time-lagged semilinear parabolic problems*, Natl. Acad. Sci. Lett. **46** (2023) 347–350.

[32] S. Priyadarshana, J. Mohapatra, S.R. Pattanaik, *An improved time accurate numerical estimation for singularly perturbed semilinear parabolic differential equations with small space shifts and a large time lag*, Math. Comput. Simul. **214** (2023) 183–203.

[33] M. Rahman, *Integral Equations and Their Applications*, WIT Press, 2007.

[34] A. Saadatmandi, M. Dehghan, *Numerical solution of the higher-order linear Fredholm integro-differential-difference equation with variable coefficients*, Comput. Math. Appl. **59** (2010) 2996–3004.

[35] S. Sevgin, *Numerical solution of a singularly perturbed Volterra integro-differential equation*, Adv. Differ. Equ. **2014** (2014) 171.

[36] S.Q. Wang, J.H. He, *Variational iteration method for solving integro-differential equations*, Phys. Lett. A **367** (2007) 188–191.